Aquaculture Reports 34 (2024) 101883

Contents lists available at ScienceDirect

Aquaculture Reports

journal homepage: www.elsevier.com/locate/aqrep

A newly isolated *Pseudomonas otitidis* phage, vB_PotS-PotUPM1 from tilapia in Malaysia

An Nie Tee [a], Megat Hamzah Megat Mazhar Khair [a], Chou Min Chong [b], Mohd Asrore Mohd Shaufi [a], Khatijah Yusoff [a,c], Hok Chai Yam [d], Han Ming Gan [e], Adelene Ai-Lian Song [a,f,*]

[a] Department of Microbiology, Faculty of Biotechnology and Biomolecular Sciences, Universiti Putra Malaysia, Serdang 43400, Selangor, Malaysia
[b] Department of Aquaculture, Faculty of Agriculture, Universiti Putra Malaysia, Serdang 43400, Selangor, Malaysia
[c] Malaysia Genome and Vaccine Institute, National Institutes of Biotechnology Malaysia, Kajang 43000, Selangor, Malaysia
[d] Department of Biotechnology, Faculty of Applied Sciences, UCSI University, Cheras 56000, Wilayah Persekutuan Kuala Lumpur, Malaysia
[e] Patriot Biotech, Subang Jaya 47500, Selangor, Malaysia
[f] Institute of Bioscience, Universiti Putra Malaysia, Serdang 43400, Selangor, Malaysia

ARTICLE INFO

Keywords:
Pseudomonas otitidis
Bacteriophage
Gram-negative pathogen
Tilapia

ABSTRACT

A new *Pseudomonas* species, *Pseudomonas otitidis* was first known as an otic infectious agent in human. The presence of an inherent metallo-β-lactamase gene and its recent emergence in aquaculture underscore its potential zoonotic pathogenicity. The present study is aimed to characterize *P. otitidis* NK1 and its bacteriophage vB_PotS-PotUPM1 (PotUPM1), which were isolated from an infected tilapia fish farm in Malaysia. *P. otitidis* NK1 showed beta-hemolysis on blood agar and is resistant to several antibiotics. Its genome size was 6067,534 bp, with an average nucleotide identity of less than 99 % to all *P. otitidis* genome assemblies in GenBank, making it a novel strain of *P. otitidis*. The phage PotUPM1 has a latent period of 45 min and a burst size of 405 phage particles per bacterium. It effectively inhibited the growth of *P. otitidis* NK1 even at a low multiplicity of infection of 0.001 up to 9-hour post-inoculation. Transmission electron microscopy showed that it has a prolate head and a long, non-contractile tail, resembling those in the *Siphoviridae* family. Based on bioinformatic analysis, PotUPM1 has no resistance or virulence genes and is a lysogenic phage based on the presence of an integrase gene in the phage genome. Similarity analysis showed that PotUPM1 may represent a novel viral species with less than 95 % nucleotide sequence similarity to other characterized phages. The findings of this study could provide an insight on the occurrence of *P. otitidis* in the aquaculture industry and lay a basis for the application of phage or phage-derived proteins against pathogenic *P. otitidis* to alleviate antimicrobial resistance.

1. Introduction

Pseudomonas otitidis is a Gram-negative pathogen that was first reported as an otic infectious agent in human (Clark et al., 2006). It is a rare species of the *Pseudomonas* genus where little were reported on its clinical significance since its first discovery in 2002 (Roland and Stroman, 2002). This bacterium also caused non otic infections such as necrotizing fasciitis (Kim et al., 2016), pan-peritonitis (Kim et al., 2016), bacteremia (Caixinha et al., 2021), pneumonia (Caixinha et al., 2021) and epididymo-orchitis (Alqurashi et al., 2022). Misidentifications of *P. otitidis* as other pathogens especially *Pseudomonas aeruginosa* are common in clinical diagnosis, as routine phenotypic testing may not accurately identity *P. otitidis* unless molecular methods are used (Alqurashi et al., 2022; Caixinha et al., 2021; Kim et al., 2016). In addition to human sources, *P. otitidis* has been found in various environmental sources such as soil (Ahn, 2018; Saber et al., 2015), water bodies (García-Ulloa et al., 2021; Miyazaki et al., 2020), wastewater (Ibrahim and Abd Elsalam, 2018; Jing et al., 2009; Naguib et al., 2019; Singh and Tiwary, 2016; Thulasinathan et al., 2019), food (Wong et al., 2015), cow (Tan et al., 2015), and fish (Husain et al., 2022; Sarjito et al., 2022), most of which were reported with environmental-friendly uses.

The present study isolated a strain of *P. otitidis* from the internal

* Corresponding author at: Department of Microbiology, Faculty of Biotechnology and Biomolecular Sciences, Universiti Putra Malaysia, Serdang 43400, Selangor, Malaysia.
E-mail address: adelene@upm.edu.my (A.A.-L. Song).

https://doi.org/10.1016/j.aqrep.2023.101883
Received 2 August 2023; Received in revised form 28 October 2023; Accepted 10 December 2023
Available online 18 December 2023

organs of dead juvenile red hybrid tilapia (*Oreochromis* spp.) obtained from a fish farm with a disease outbreak in Semenyih, Selangor, Malaysia. The potential pathogenicity of *P. otitidis* in animals has not been reported despite its pathogenicity in human. The underrepresentation of *P. otitidis* in the aquaculture industry may be due to its genotypic and phenotypic similarities with *P. aeruginosa*, a well-established opportunistic pathogen in aquaculture. Recently, a male patient diagnosed with epididymo-orchitis caused by *P. otitidis* had a history of tilapia consumption prior to the onset of his symptoms (Alqurashi et al., 2022), suggesting that *P. otitidis* may be a zoonotic pathogen. Antibiotics are the drug of choice for the current treatment of *P. otitidis* infections in human. However, all *P. otitidis* are endowed with a resident metallo-β-lactamase (MBL) gene, a species-related trait with unusual β-lactams antibiotic susceptibility (Lee et al., 2012; Thaller et al., 2011). The potential of *P. otitidis* as a zoonotic bacterial pathogen in addition to its antibiotic resistance calls for the development of antibiotic alternatives to tackle the emergence of this pathogen in aquaculture.

As natural killers of bacteria, bacteriophages are promising tools to combat the pathogenic bacteria. Bacteriophages, or phages in short, are viruses that infect and replicate in bacteria. Phages exhibit two different life cycles within their bacterial hosts, lytic and lysogenic (Harada et al., 2018). The ability to lyse bacteria without integration into the host chromosome has led to the use of strictly lytic phages for phage therapy as antimicrobial treatment for bacterial infections in the last century (Ghose and Euler, 2020). Apart from antimicrobial therapy, phages are also applied for various uses such as gene delivery, food safety, biocontrol of plant pathogens, phage display, biosensing devices, and surface disinfectants (Rogovski et al., 2021).

While isolation of phages targeting *Pseudomonas* spp. are frequently reported (Chegini et al., 2020), no phage against *P. otitidis* has been reported to date. In this context, a phage that was co-isolated with its host, *P. otitidis* from a dead tilapia in this study offers a potential antimicrobial alternative in line with the natural bacterial killing ability of bacteriophage. Furthermore, the significance and pathogenicity of *P. otitidis* isolated from aquaculture is severely lacking in literature. To date, there have only been three reports of *P. otitidis* isolated from fish, including freshwater ornamental fish species imported into North America from Colombia, Singapore, and Florida (Rose et al., 2013), marine fish, *Moolgarda seheli* in India (Husain et al., 2022), and freshwater giant gourami, *Osphronemus goramy* in Indonesia (Sarjito et al., 2022). Due to this, here we report a comprehensive study on the phenotypic and genotypic characterization of *P. otitidis* strain NK1 and its phage, denoted vB_PotS-PotUPM1 (a **v**irus of **B**acteria, infecting ***P**seudomonas **o**titidis*, with **s**iphovirus morphology, named PotUPM1), referred to herein as PotUPM1. It is expected that with this study, the role and implications of *P. otitidis* in the aquaculture setting will be better defined.

2. Materials and methods

2.1. Bacterial strains and growth conditions

Apart from the reference strains from German Collection of Microorganisms and Cell Cultures GmbH (DSMZ) and American Type Culture Collection (ATCC), a total of 18 bacterial strains including *P. otitidis* NK1 used in this study were isolated from tilapia farms in Selangor, Malaysia. All strains were cultured in Luria-Bertani (LB) broth (Millipore, US) or plated on LB agar (Millipore, US), except *Streptococcus pyogenes* that was cultured in brain heart infusion (BHI) broth or agar plates (Millipore, US). *P. otitidis* NK1 was grown on blood agar for the identification of hemolysis type. The liquid cultures were grown at 37 °C in a shaking incubator at a rate of 200 rpm, and the agar plates were incubated at 37 °C overnight. Preservation of the strains was done using 25 % glycerol stocks stored at –80 °C.

2.2. Antimicrobial susceptibility test of P. otitidis NK1

The antibiotic resistance of *P. otitidis* NK1 to different groups of antibiotics were determined using the Kirby-Bauer disk diffusion method according to the Clinical and Laboratory Standards Institute (CLSI) guidelines M100 (CLSI, 2021). The antibiotic discs (Oxoid™, UK) used were aminoglycoside (gentamicin, GM/10 μg), carbapenems (doripenem, DOR/10 μg; imipenem, IPM/10 μg; meropenem, MEM/10 μg), cephalosporins (cefepime, FEP/30 μg; ceftazidime, CAZ/30 μg), fluoroquinolones (ciprofloxacin, CIP/5 μg; norfloxacin, NOR/10 μg), monobactam (aztreonam, ATM/30 μg), penicillin (piperacillin, PRL/100 μg), and tetracycline (minocycline, MH/30 μg). The respective antibiotic discs were placed on Mueller-Hinton agar (Millipore, United States) plates inoculated with a pure culture of the bacterium. After incubation at 37 °C for 18 h, the inhibition zones formed were measured and compared with the critical values of CLSI to determine whether the bacterium is susceptible, intermediate, or resistant (CLSI, 2021). *P. aeruginosa* ATCC 27853 was used as the quality control strain.

2.3. Isolation and concentration of phage vB_PotS-PotUPM1

Phage vB_PotS-PotUPM1 (PotUPM1) was isolated from a dead juvenile tilapia sample collected from a fish farm in Selangor, Malaysia using spot test and double-layer agar method, as previously described with some modifications (Clokie et al., 2009). *P. otitidis* NK1 that was isolated from the same source was used as the propagation host. In brief, the fish sample was surface sterilised, crushed and suspended in phage SM buffer (100 mM NaCl, 8 mM $MgSO_4{\cdot}7\ H_2O$, 50 mM Tris-HCl, and 0.01 % (w/v) gelatine). The mixture was centrifuged at 7000 ×*g* for 10 min and filtered through a 0.22 μm membrane filter (Millipore, US) to remove bacteria and fish debris. A mid-log phase *P. otitidis* NK1 culture ($OD_{600\ nm} \sim 0.5$) was added to the filtrate and incubated at 37 °C overnight with shaking for enrichment. The subsequent enrichment culture was centrifuged and filtered through a 0.22 μm membrane filter. The presence of phage infecting *P. otitidis* NK1 in the supernatant was screened through a spot test by spotting 10 μL of the clarified phage suspension on LB agar containing a lawn of *P. otitidis* NK1. The clearance of the lawn in the spot indicated the presence of phage against *P. otitidis* NK1. To isolate pure phages, streak plate purification was performed according to the protocol described by Cross et al. (2015) with minor modifications. Briefly, a sterile pipette tip was dipped into the clear zone and streaked on a LB agar plate (1.5 % (w/v) agar with 1 mM $CaCl_2$) using a quadrant streaking method, followed by the addition of molten LB agar (0.7 % (w/v) agar with 1 mM $CaCl_2$) containing *P. otitidis*. Plaque purification was repeated three times by picking a single plaque until homogenous plaques were obtained. For the determination of plaque morphology and titre, the phage suspension from an individual plaque was tested for plaque formation with *P. otitidis* NK1 by double-layer agar method, consisting of LB medium with a bottom layer (1.5 % (w/v) agar) and a top layer (0.7 % (w/v) agar) with 1 mM $CaCl_2$ (Clokie et al., 2009). In brief, 100 μL of the phage suspension and 100 μL of mid-log phase bacteria were mixed and incubated at room temperature for 10 min. The phage-bacteria suspension was then added to the molten top layer agar and poured onto plates containing the bottom layer agar. The double-layer agar plates were incubated overnight at 37 °C for plaque formation. The next day, the number of plaque-forming unit (PFU), plaque morphology and plaque diameter were determined. To obtain high titre phage suspension, double-layer agar plates with confluent lysis (~3000 PFUs) were flooded with SM buffer and rocked overnight at 4 °C. Phage suspensions were pooled from the plates, and then centrifuged at 7000 ×*g* for 10 min and filtered through a 0.22 μm membrane filter (Millipore, US). The filtrate was then concentrated by precipitation with 1 M NaCl and 10 % PEG-8000 (Kwiatek et al., 2017). The clarified supernatant containing high titre phage suspension was stored at 4 °C until further analysis.

2.4. Transmission electron microscopy analysis

For transmission electron microscopy (TEM) analysis, the phage suspension (10^{13} PFU/mL) was further purified using caesium chloride (CsCl) gradient ultracentrifugation with densities of 1.4 g/cm^3, 1.5 g/cm^3, and 1.6 g/cm^3. The samples were centrifuged at 67,200×*g* for 3 h at 4 °C in a Class S ultracentrifuge using SW 40 Ti Swinging-Bucket Rotor (Beckman Coulter Inc., Brea, CA, USA) at the Microscopy Unit, Institute of Bioscience, Universiti Putra Malaysia. The phage band was collected, dialysed with SM buffer twice, and stored at 4 °C. The purified phage stock was washed with 0.1 M neutral ammonium acetate. A drop of the suspension was placed on a grid and negatively stained using 2 % uranyl acetate (pH 4–4.5). The morphology of the phage particles was observed using the JEM21000F TEM, 200 kV Field Emission (JEOL, Tokyo, Japan) as described previously (Ackermann, 2012).

2.5. Phage lytic spectrum analysis

Spot tests were performed to determine the host range of phage PotUPM1. Phage suspension (~10^7 PFU/mL) was spotted on a double-layer agar containing a lawn of the appropriate bacteria strains. SM buffer was also spotted as a negative control. The plates were incubated overnight at 37 °C and the appearance of clear lysis zones indicating the lytic activity of the phage was recorded.

2.6. Bacterial growth inhibition assay

The effect of phage on the growth of *P. otitidis* NK1 was investigated via a bacterial growth inhibition assay performed in a 96-well microplate, as previously described with slight modifications (Lerdsittikul et al., 2022). Phage suspension (10^8 PFU/mL) was mixed with *P. otitidis* NK1 at mid-log phase at multiplicity of infection (MOI) of 10, 1, 0.1, 0.01, and 0.001 (in triplicates) and the microplates were incubated at 37 °C. Bacterial culture without phage was used as a growth control. The bacterial growth was measured by taking the absorbance (OD_{600}) reading using iMark™ Microplate Reader (Bio-Rad, Hercules, CA, USA) every 30 min until the 9th hour. The experiment was performed in triplicates.

2.7. Phage adsorption assay and one-step growth curve analysis

The kinetics of phage adsorption to *P. otitidis* NK1 was determined according to methods described by Kropinski (2009) with slight modifications. In brief, mid-log phase *P. otitidis* NK1 in LB broth was mixed with the phage suspension (~10^7 PFU/mL) at a MOI of 0.1 and incubated at 37 °C. Aliquots were collected at 0, 10, 15, 20, 30, 45 min post-inoculation and centrifuged immediately at 4 °C to sediment the bacterial cells and the adsorbed phages. The supernatants were serially diluted and the titres of free, unadsorbed phage particles were determined using double-layer agar method. One-step growth curve assay was performed as described previously with some modifications (Hyman and Abedon, 2009). Briefly, mid-log phase *P. otitidis* NK1 was added with the phage suspension (~10^7 PFU/mL) at MOI of 0.1 and incubated for 10 min at 37 °C. The mixture was then centrifuged at 4 °C to remove the unadsorbed virion particles. The pellets containing the infected cells were resuspended in 10 mL of pre-warmed LB broth and incubated at 37 °C. Aliquots were taken every 15 min for 90 min. The phage titres were determined using double-layer agar method. A one-step growth curve was plotted based on the titre calculated over time to observe the latent period, and the phage burst size was calculated by dividing the phage titre at the end by the titre at the beginning of the experiments. These experiments were performed in triplicates.

2.8. Lysogeny assay

The lysogenic efficiency of phage PotUPM1 was determined via a lysogeny assay as described by Nasr Azadani et al. (2020) with slight modifications. In brief, 100 μL of phage suspension (10^9 PFU/mL) was seeded on five LB agar plates. A mid-log phase culture of *P. otitidis* NK1 was serially diluted up to 10^{-9} and 100 μL aliquots of the bacterial dilutions of 10^{-5} to 10^{-9} were plated onto the phage seeded plates, respectively. The same bacterial dilutions were also plated onto five unseeded plates as a negative control. The plates were incubated at 37 °C for 48 h. The lysogenic efficiency was calculated by dividing the number of bacterial colonies formed on the phage seeded plates by the number of colonies on the unseeded plates and multiplying the quotient by 100.

2.9. Temperature and pH stability of phage PotUPM1

Phage tolerance to pH and heat were determined according to the methods described by Decewicz et al. (2020). For the measurement of phage stability at high temperature, the phage suspensions (10^8 PFU/mL) were incubated at 50 °C, 60 °C, 70 °C, and 80 °C separately for 1 h, where samples were collected at the 10th minute and 60th minute. For pH stability, phage suspensions (10^8 PFU/mL) in LB broth were incubated at different pH ranging from 3 to 12 at 37 °C for 2 h. Phage titres for each test were determined using the double-layer agar method. The experiments were performed in triplicates.

2.10. Whole genome sequencing of P. otitidis NK1 and phage PotUPM1

The genomic DNA of *P. otitidis* NK1 was extracted using Biospin Bacteria Genomic DNA Extraction Kit (Bioer, China). Phage genomic DNA was extracted from phage suspension (10^{13} PFU/mL) using the phenol-chloroform method (Green and Sambrook, 2017). The genomic DNA was sent to Apical Scientific Sdn Bhd (Selangor, Malaysia) for sequencing. For library construction, the genome DNA was randomly trimmed into short fragments, followed by end repairing, A-tailing, and ligating with Illumina adapters. The fragments with adapters were amplified using PCR and purified. For quantification and detection of size distribution, the library was tested using Qubit and real-time PCR. The quantified libraries were pooled and sequenced on Illumina platforms. Whole genome sequencing was performed on a NovaSeq 6000 system using 150 bp paired-end chemistry. For genome assembly, the raw reads were trimmed using bbduk of the BBTools Packages (https://jgi.doe.gov/data-and-tools/bbtools/) to remove the Illumina adapter sequences. The filtered reads were assembled de novo and polished using Spades v3.13 (Kolmogorov et al., 2019) and Pilon v1.23 (Walker et al., 2014), respectively as implemented in Unicycler 0.4.8 (Wick et al., 2017).

2.11. Bioinformatic analysis of P. otitidis NK1

Genome annotation of *P. otitidis* NK1 was performed using PATRIC annotation tool v.3.6.12 and Rapid Annotation using Subsytems Technology (RAST) server v.2.0 using the assembled whole genome (Davis et al., 2020; Overbeek et al., 2014). Antimicrobial resistance genes and virulence factors in the bacterial genome were identified using ResFinder 4.0, Comprehensive Antibiotic Resistance Database (CARD) and Virulence Factor Database (VFDB) in addition to the functional annotation data generated from the RAST annotation pipeline (Alcock et al., 2020; Bortolaia et al., 2020; Liu et al., 2022). The evolutionary relationship between *P. otitidis* NK1 and 22 other *P. otitidis* strains, and several representative genomes of *Pseudomonas* spp. were determined through the codon tree method in the PATRIC platform (Davis et al., 2020). Figtree v.1.4.3 software was used to view the tree and annotation of the Newick result file generated. The phylogenetic tree generated was labelled according to the names of the PATRIC genomes. Based on the phylogeny obtained, the average nucleotide identity (ANI) of the studied strains were calculated by comparing the assembled genome of *P. otitidis* NK1 with the publicly available, closely related whole genome assembly

and other representative genome in the *P. aeruginosa* group using the JSpeciesWS online platform (Richter et al., 2016).

2.12. Bioinformatic analysis of phage PotUPM1

Open reading frames prediction and functional annotation of the assembled phage genome were done using RAST and eggNOG-mapper platforms (Cantalapiedra et al., 2021; Overbeek et al., 2014). The antimicrobial resistance genes in the phage genome were identified using the CARD server (Alcock et al., 2020). In addition, PhageLeads was used to predict the lifestyle of the phage (Yukgehnaish et al., 2022). For visualization of the phage whole genome, a circular genome map was generated using Snapgene (http://www.snapgene.com/). The whole genome sequence was queried against the viruses (TaxID:10239) nucleotide collection (nr/nt) using BLASTn to search for similar sequences. A proteomic tree was generated by the ViPTree server based on genome-wide sequence similarities computed by tBLASTx (Nishimura et al., 2017). A total of 2891 related viral sequences were selected to build the proteomic tree, and 19 selected genome sequences with highest all-against-all genomic similarity (S_G) scores were selected to draw a rectangular proteomic tree using VIPTree version 3.4 (Nishimura et al., 2017).

2.13. Statistical analysis

Statistical analyses of the data were performed using the GraphPad Prism software version 9. One-way ANOVA with repeated measures was used to analyse the significant differences in phage titres in the pH stability experiment. Two-way ANOVA with repeated measures was applied to evaluate the significant differences in the thermal stability experiment with two different incubation length and the bacterial growth inhibition assay upon phage infection at different MOIs. The significance of the differences between the experimental groups was considered at $P \leq 0.05$.

3. Results

3.1. Colony morphology, hemolytic phenotype, and antimicrobial resistance profile of P. otitidis NK1

P. otitidis NK1 showed yellow-green colored colonies on Luria-Bertani agar (Supplementary Fig. S1 A), resembling *P. aeruginosa*. *P. otitidis* NK1 was grown on blood agar to determine its ability to cause blood hemolysis, which is commonly related to pathogenicity. The bacterial colonies showed complete clearing on blood agar, indicating the beta-hemolytic activity of *P. otitidis* NK1 (Supplementary Fig. S1 B). In terms of its susceptibility to antibiotics, *P. otitidis* NK1 was tested with 11 antibiotics from seven classes. The Kirby-Bauer antibiotic susceptibility test results were interpreted according to the Clinical & Laboratory Standards Institute (CLSI) breakpoints for *P. aeruginosa* because of their similar phenotypic and genotypic characteristics (CLSI, 2021; Thaller et al., 2011). *P. otitidis* NK1 was resistant to meropenem, but had intermediate resistance to doripenem, aztreonam and minocycline, and was susceptible to the remaining antibiotics tested (Table 1). As minocycline's breakpoints were not specified in the CLSI breakpoints for *P. aeruginosa,* the breakpoints for other Gram-negative bacilli were used as reference.

As the phenotypic characterization of the antibiotic resistance patterns of *P. otitidis* NK1 showed that it was resistant to several clinically important antibiotics, the antimicrobial resistance genes within the genome of *P. otitidis* NK1 was also identified by functional annotation platforms to further establish its potential resistance behaviour. Four antimicrobial genes were identified in the genome of *P. otitidis* NK1, which were bla_{POM-1}, *adeF*, *qacG* and *rsmA* that confer resistance to several types of antimicrobials through either inactivation or efflux of antibiotic (Table 2). However, in in vitro experiments, *P. otitidis* NK1 was found to be susceptible to some of the antibiotics listed in Table 1, such as cefepime, imipenem, ceftazidime, and fluoroquinolone. In addition to the antimicrobial genes, genes putative for important virulence factors such as adherence, anti-phagocytosis, iron uptake system, secretion systems, efflux pump, and toxin production were also found in the genome of *P. otitidis* NK1 (Table 2).

Table 1
Antibiotic susceptibility profile of *P. otitidis* NK1 to seven classes of antibiotics.

Antibiotic class	Antibiotics	Zone of inhibition ± standard deviation (mm)	Antibiotic Susceptibility Test Results
Aminoglycoside	Gentamicin (GM/10 μg)	25.5 ± 0.5	S
Carbapenem	Doripenem (DOR/10 μg)	17.5 ± 0.5	I
	Imipenem (IPM/10 μg)	26.8 ± 0.8	S
	Meropenem (MEM/10 μg)	7.0 ± 0	R
Cephalosporin	Cefepime (FEP/30 μg)	30.7 ± 0.57	S
	Ceftazidime (CAZ/30 μg)	28.5 ± 0.5	S
Fluoroquinolone	Ciprofloxacin (CIP/5 μg)	41.3 ± 0.3	S
	Norfloxacin (NOR/10 μg)	37.8 ± 1.0	S
Monobactam	Aztreonam (ATM/30 μg)	20.0 ± 0	I
Penicillin	Piperacillin (PRL/100 μg)	27.0 ± 0	S
Tetracycline	Minocycline (MH/30 μg)	14.5 ± 0.5	I

* S = Susceptible, I = Intermediate; R = Resistant.

3.2. Whole genome analysis and phylogeny of P. otitidis NK1

The genome assembly of *P. otitidis* NK1 was 6067,534 bp in size and consisted of 34 contigs with a GC content of 67 %. The number of coding sequences (CDS) detected was 5718, with 57 tRNA and 3 RNA non-coding sequences. For genome annotation, there were 4238 functionally assigned proteins and 1480 hypothetical proteins (Fig. 1A). Most of the annotated genes belong to the subsystems involved in amino acid, protein metabolism, carbohydrates, and cofactors, vitamins, prosthetic group and pigments, which comprise the four largest functional categories in the chart shown in Fig. 1B.

A comparative analysis of the phylogeny showed that *P. otitidis* NK1 and several *P. otitidis* strains available in the PATRIC database belong to the same clade (Fig. 2). To establish the phylogenetic relationship of *P. otitidis* NK1 further, pairwise average nucleotide identity based on BLAST+ (ANIb) values were calculated by comparing genome assembly of *P. otitidis* NK1 with all four complete genome assemblies of *P. otitidis* species available in Genbank database, one reference strain from the German Collection of Microorganisms (DSM), and three representative genomes of the *P. aeruginosa* group members (Table 3). The calculated ANI values support the clusters in the phylogenetic tree. Strain NK1 had ANI values of more than 97 % for all four genome assemblies of *P. otitidis* strains, which were strains BC12, MrB4, WP8-S17-CRE-03, and CSMC7.1 that were isolated in Ghana, Japan, and Hong Kong. Based on the ANI value cutoff at ≥ 99.00 % for strains and ≥ 96.50 % for species (Girard et al., 2021), the strain isolated in the present study was shown to be a novel strain of *P. otitidis*.

3.3. Isolation and characterization of phage PotUPM1

P. otitidis NK1 and phage PotUPM1 were both isolated from the same source, which was a dead juvenile red hybrid tilapia, *Oreochromis* sp. from a fish farm located in Selangor, Malaysia during a disease outbreak.

Table 2
Antimicrobial resistance genes and virulence classes found in the genome of *P. otitidis* NK1.

Resistance gene	Antimicrobial resistance gene family	Drug class	Resistance mechanism
bla$_{POM-1}$	POM-1 β-lactamase	β-lactam (ampicillin, amoxicillin + clavulanic acid, cefoxitin, piperacillin, amoxicillin, meropenem, cefepime, piperacillin + tazobactam, imipenem, cefixime, ceftazidime, ampicillin + lavulanic acid, cefotaxime, ertapenem)	Antibiotic inactivation
adeF	Resistance-nodulation-cell division (RND) antibiotic efflux pump	Fluoroquinolone, tetracycline	Antibiotic efflux
qacG	Small multidrug resistance (SMR) antibiotic efflux pump	Disinfecting agents and antiseptics	Antibiotic efflux
rsmA	Resistance-nodulation-cell division (RND) antibiotic efflux pump	Fluoroquinolone, diaminopyrimidine, phenicol	Antibiotic efflux
Virulence class		**Virulence factors**	
Adherence		Flagella, lateral flagella, polar flagella, lipopolysaccharide O-antigen, type IV pili biosynthesis, type IV pili twitching motility related proteins	
Anti-phagocytosis		Alginate biosynthesis and regulation, capsular polysaccharide	
Enzyme		Phospholipase C and non-hemolytic phospholipase C, protease (elastase)	
Iron uptake		Salmochelin, pyoverdine, pyoverdine receptors	
Regulation		GacS/GacA two-component system	
Secretion system		EPS type II secretion system (T2SS), type III secretion system (T3SS) effectors, hcp secretion island-1 encoded type VI secretion system (H-T6SS)	
Toxin		Phaseolotoxin	
Efflux pump		MtrCDE	

Using *P. otitidis* NK1 as host, phage PotUPM1 produced moderate size plaques of about 3 mm in diameter with clear centers and turbid edges on a double-layer agar (Fig. 3A).

Transmission electron microscopy imaging showed that phage PotUPM1 had a slightly prolate head with a diameter of 66.3 ± 5.3 nm, and a long, non-contractile tail with a length of 112.3 ± 19.0 nm (Fig. 3B). The tail structure is typical of the members of siphovirus. The analysis of whole genome sequencing also revealed that the phage is a double-stranded DNA virus. Therefore, phage PotUPM1 was classified as a member of *Siphoviridae* in the order of Caudovirales and named as vB_PotS-PotUPM1 according to the current nomenclature guidelines, as described by Adriaenssens and Brister (2017).

3.4. Host range of phage PotUPM1

Host spectrum of phage PotUPM1 was evaluated using spot test against bacteria representing different genera from various sources (Supplementary Table S1). Although phage PotUPM1 was enriched from tilapia sample using *P. otitidis* NK1 as a host, it did not exhibit any lytic activity against the other bacterial isolates from the same farm. Phage PotUPM1 also showed no lytic activity on any of the other laboratory and environmental strains tested, including the only available *P. otitidis* reference strain, DSM17224. This preliminary result suggests that the phage PotUPM1 has a narrow host range and is very specific to the *P. otitidis* strain isolated.

3.5. Thermal tolerance and pH stability

The investigation of phage stability at various temperatures and pH are important for the propagation, storage, and subsequent downstream experiments. The thermal tolerance of phage PotUPM1 were tested from 40 °C to 70 °C with 10 °C intervals, and aliquots were taken at the 10th and 60th minute post-incubation. Phage PotUPM1 was relatively stable from 40 °C to 60 °C after 10 min incubation (Fig. 4A). However, after prolonged incubation up to 1 h, there was a slight but statistically significant phage titre drop ($P \leq 0.01$) at 40 °C but remained stable at 50 °C and 60 °C. When exposed to 70 °C, phage PotUPM1 was completely inactivated even after 10 min of incubation. For pH stability, phage PotUPM1 showed similar stability from pH 4–12 and no viability at the extreme pH of 3 and 13 (Fig. 4B).

3.6. Growth kinetics of phage PotUPM1

Phage growth kinetics were determined by the adsorption and one-step growth assay that define the adsorption rate, latent period, eclipse period, and burst size. The adsorption curve of phage PotUPM1 showed that about 25 % of the phage particles were attached to the host cells, *P. otitidis* NK1 within 10 min (Fig. 5A). The maximum percentage of phage attached to hosts was 75 % at 45-minute post-inoculation. The adsorption efficiency was constant throughout the tested period. Based on the one-step growth curve of phage PotUPM1 infecting *P. otitidis* NK1, it had a latent period of about 45 min and a burst size of approximately 405 PFU/cell, which was consistent with the typical pattern of a tailed phage (Fig. 5B). Despite its large burst size, phage PotUPM1 exhibited a low rate of adsorption to the surface of its host cells and a moderate latent period. The phage adsorption to host cells was slow even though an actively growing bacterial culture (log phase) was used.

The killing activity of phage PotUPM1 on its host cells in broth medium were further investigated. The bacterial lysis activity of phage PotUPM1 at various multiplicity of infections (MOIs) were monitored by measuring the absorbance (OD_{600}) during phage infection. When different MOIs were used for the killing assay, there was a significant difference in bacterial growth ($P \leq 0.0001$), indicating that the higher the MOI used, the better the killing efficiency of the phage. At higher MOIs (10 and 1), the absorbance reading of the cultures showed a slight reduction upon infection and remained low up to 9-hour post-inoculation. In contrast, the absorbance of the cultures at lower MOIs (0.1, 0.01, 0.001) first increased after infection up to 2- to 3.5-hour post-inoculation and decreased to a minimum at 9-hour post-inoculation (Fig. 5C). The absorbance value of *P. otitidis* NK1 incubated with phage PotUPM1 at MOI of 0.001, 0.01, 0.1, 1, and 10 were significantly lower than the growth control at a MOI of 0 ($P \leq 0.0001$), starting from 4-hour post inoculation. This growth inhibition assay showed that higher phage concentrations (10^8-10^9 PFU/mL) at higher MOI were able to inhibit bacterial growth at the start of the infection process while low phage concentrations (10^5-10^7 PFU/mL) caused bacterial growth inhibition after at least 2 h of infection. Overall, all absorbance readings (except positive control containing bacteria only) remained low until 9-hour post-inoculation, suggesting that phage PotUPM1 could effectively inhibit the growth of *P. otitidis* NK1 even when a low MOI of 0.001 was used.

3.7. Genome analysis of phage PotUPM1

The sequence analysis from Phaster revealed that phage PotUPM1 has a circular genome of 35,685 bp in length (coverage of 71.44×) and a GC content of 66.59 %. The GC content is similar to that of *P. otitidis* NK1 (67 %), consistent with the general trend of phages that have GC content similar to that of their natural host (Almpanis et al., 2018). The genome of phage PotUPM1 has a total of 53 CDS, where 19 of them are annotated

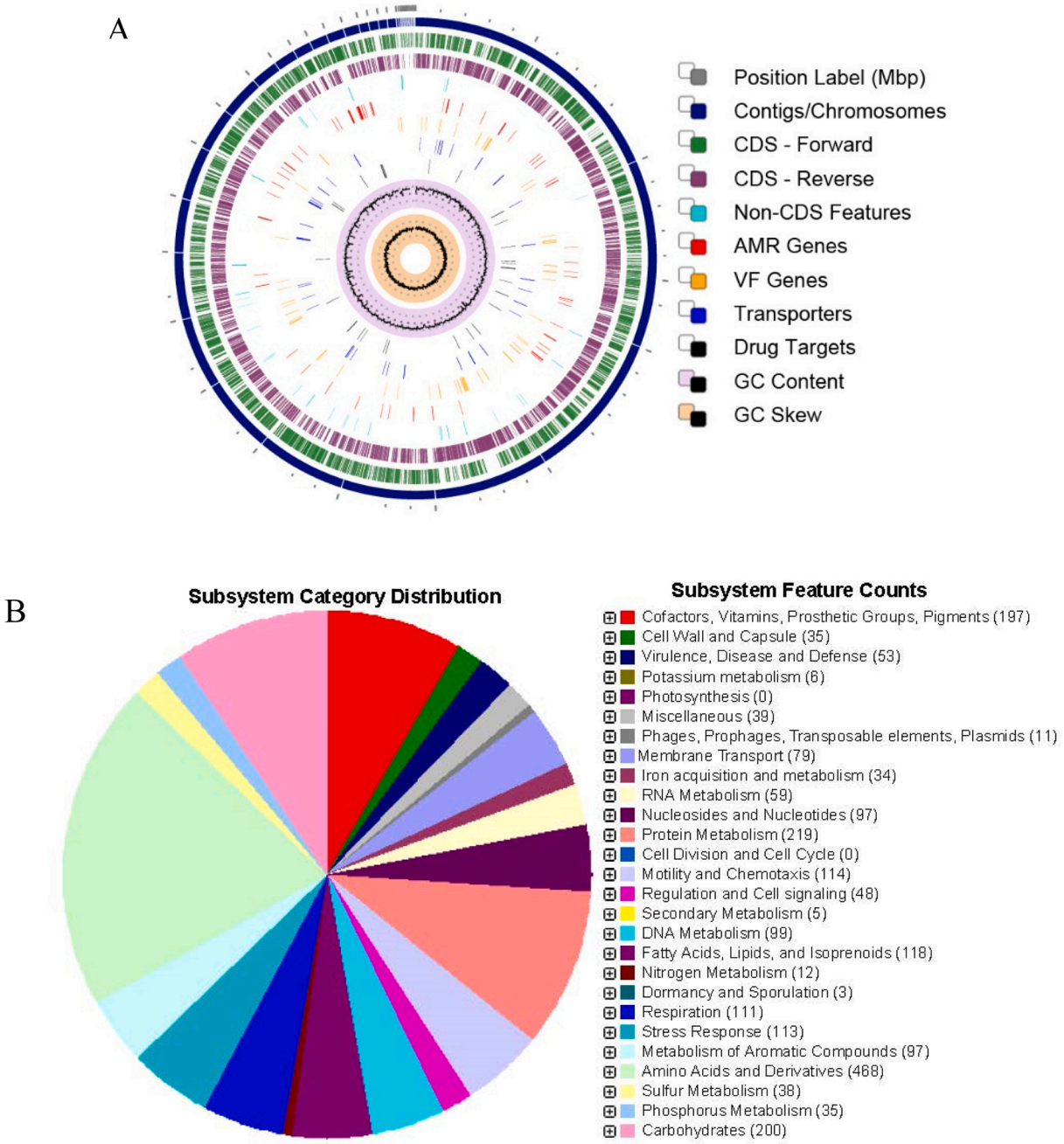

Fig. 1. Circular schematic diagram of *P. otitidis* NK1 genome generated through PATRIC and RAST platform. (**A**) A genome map of *P. otitidis* NK1 showing the overall gene characteristics; (**B**) A pie chart showing the subsystem category distribution of the annotated genes with their respective functional classifications.

with specific functions and 34 of them are hypothetical proteins. A putative phage attachment site was also detected by Phaster. A gene encoding for phage integrase was found in the PotUPM1 genome, indicating that the phage may be a lysogenic phage. The PhageLeads result confirmed that this phage has a temperate lifestyle cycle with no antimicrobial resistance or virulence genes. However, the lysogenic efficiency of phage PotUPM1 on *P. otitidis* NK1 calculated in the in vitro experiment was 0 % (lytic efficiency is 100 %) as shown in Supplementary Table S2, indicating that the phage was lytic against *P. otitidis* NK1 under normal laboratory phage propagation conditions.

The gene annotation information of phage PotUPM1 was shown in Supplementary Table S3. Most genes are on the minus strand (43 CDS) while only 10 were on the plus strand. The circular genome map with annotated gene products and their functional groups are shown in Fig. 6.

The CDS are divided into several functional groups based on Clusters of Orthologous Groups (COGs) as follows:

(i) Replication, recombination, and repair

DNA replication, recombination and repair are the essential processes involved in the transmission of genetic information within and between generations. The genome of phage PotUPM1 encodes for several proteins involved in these processes, such as adenine-specific methyltransferase, DNA methylase, phage integrase, and phage terminase (small subunit).

(ii) Cell wall/membrane/envelope biogenesis

Only one coding sequence was categorized under this functional group, which is a gene encoding for tape measure protein. It determines the length of the phage's tail and facilitates the

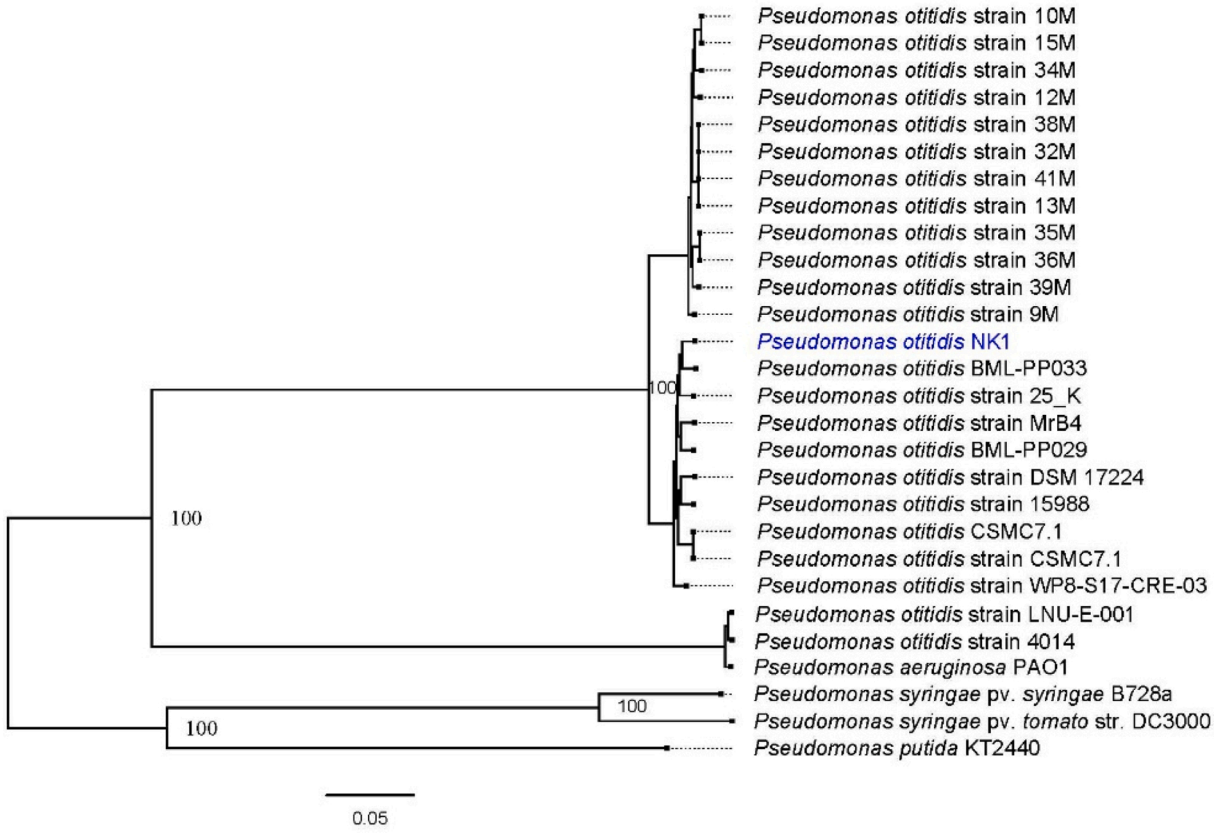

Fig. 2. The phylogenetic tree displaying the evolutionary relationship of *P. otitidis* NK1 and other selected *Pseudomonas* species based on whole genome sequences.

Table 3
Average nucleotide identity based on BLAST+ (ANIb) of *P. otitidis* NK1 and other closely related *Pseudomonas* species.

Bacteria pair	ANIb value (%)
P. otitidis NK1: *P. otitidis* BC12	98.07
P. otitidis NK1: *P. otitidis* MrB4	97.96
P. otitidis NK1: *P. otitidis* WP8-S17-CRE-03	97.96
P. otitidis NK1: *P. otitidis* DSM 17224	97.84
P. otitidis NK1: *P. otitidis* CSMC7.1	97.80
P. otitidis NK1: *P. tohonis* TUM18999	84.58
P. otitidis NK1: *P. alcaligenes* NEB 585	78.38
P. otitidis NK1: *P. aeruginosa* PAO1	78.01

transit of DNA to the host cell cytoplasm during infection. The length of this gene usually corresponds to the length of the phage's tail (Belcaid et al., 2011).

(iii) Transcription

Three gene products were involved in transcription of PotUPM1, which are phage terminase (large subunit), DNA-binding transcription factor, and peptidase S24-like. Phage terminase is responsible for DNA recognition and initiation of DNA packaging while the transcription factor controls the rate of transcription from DNA to messenger RNA.

(iv) Defence mechanisms

The gene encoding for endonuclease was classified under the defence mechanisms of phage. It is a HNH endonuclease that nicks double stranded DNA from 3 to 5 bp in the presence of a divalent metal ion with a conserved catalytic HNH motif and a zinc-binding site. HNH endonuclease gene in phage genomes is usually located next to a terminase gene, which is consistent with the pattern seen in PotUPM1. This highly conserved gene suggests a possible role in homologous recombination by nicking DNA that enhances gene conversion (Zhang et al., 2017).

(v) Unclassified

Several genes that are commonly found in phage genomes were classified as genes with unknown functions in eggNOG-mapper. Although these gene products are common phage proteins with known functions in the NCBI database, they remain incompletely characterized in the COG database and are therefore classified as genes with unknown function. These include phage gp6-like head-tail connector protein, major capsid protein, phage capsid and scaffold, portal protein, putative 3TM holin, putative phage holin, antitermination protein Q, RecA-dependent nuclease, and chitinase, an endolysin from glycoside hydrolase family.

Nucleotide comparison of the phage PotUPM1 whole genome using BLASTn with the virus nucleotide collection filter (TaxID: 10239) and program selection for somewhat similar sequences (BLASTn) generated three top hits with identity of more than 80 %, but with only less than 10 % query coverage, which were *Pseudomonas* phage LKA5 with 83.54 % identity and 7 % coverage, *Pseudomonas* phage PP9W with 83.08 % identity and 9 % coverage, and *Pseudomonas* phage Dobby with 81.03 % identity and 5 % coverage. All three top hits were *Pseudomonas* phage, but the low identity percentage and even lower percent coverage indicates that PotUPM1 may represent a novel viral species with less than 95 % nucleotide sequence similarity with other characterized phage (Adriaenssens and Brister, 2017). After removing the virus nucleotide filter in BLASTn search, a top hit, *P. otitidis* MrB4 DNA, complete genome (GenBank accession number: AP022642.1) was generated with 96.31 % identity and 31 % query cover to phage PotUPM1, suggesting that phage PotUPM1 may be a prophage in other strains of *P. otitidis*. The phylogeny of PotUPM1 was further compared with other published phages using viral proteome of whole genomes. A phylogenetic tree based on viral proteome constructed by ViPTree is shown in Fig. 7A, and the 29 closest

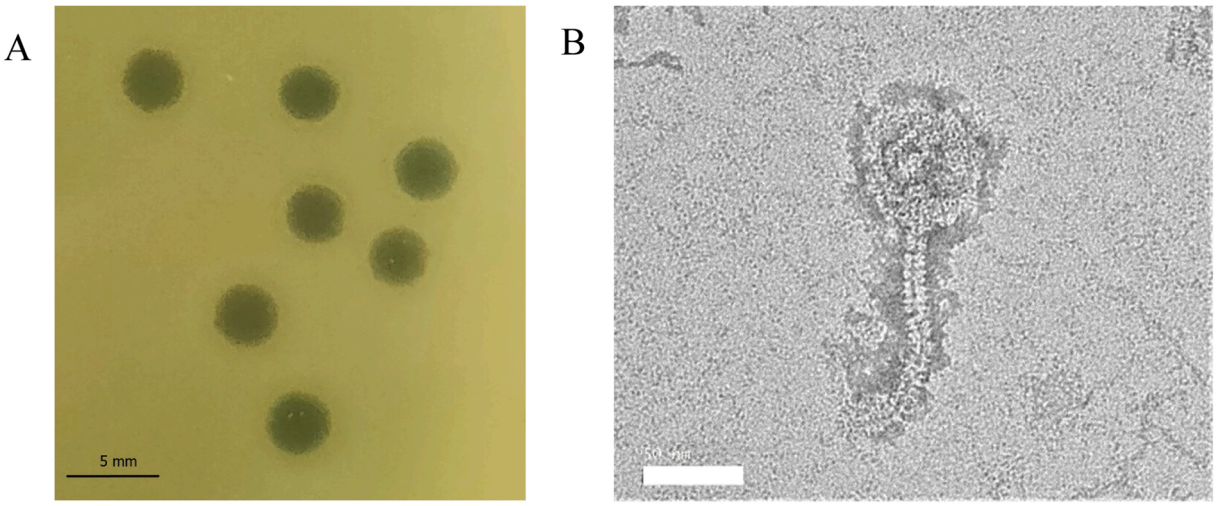

Fig. 3. Morphologies of plaque and virion of phage PotUPM1. (**A**) The plaques were circular in shape with a turbid edge on a double-layer agar plate; (**B**) The image of transmission electron microscopy showed a slightly elongated head (66.3 ± 5.3 nm) with a long tail (112.3 ± 19.0 nm). The sizes of the head diameter and tail length were represented as averages (± standard deviations) of three randomly picked phage particles. The scale bar represents 50 nm.

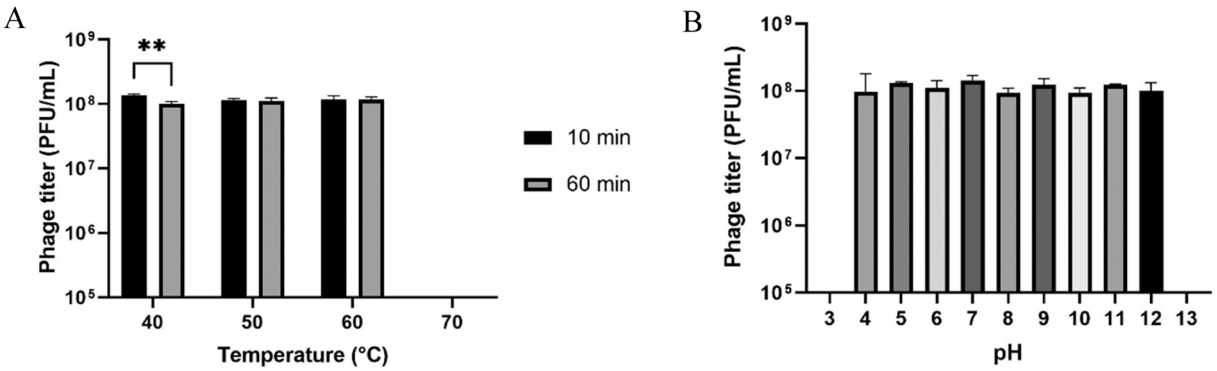

Fig. 4. Characterization of phage PotUPM1 stability at various temperature and pH conditions. **(A)** Stability of phage PotUPM1 under different high temperatures; **(B)** Phage PotUPM1 stability under different pH conditions. Data are presented as mean ± SD of three independent experiments. The asterisks indicate significant differences (** $P \leq 0.01$, two-way ANOVA) between the groups tested.

phage sequences in the tree were selected for further comparison in Fig. 7B. Based on Fig. 7B, the closest relatives of phage PotUPM1 are *Pseudomonas* phage phi2, MD8, and F10, all of which belong to the *Siphoviridae* family.

4. Discussion

As a promising growth sector in aquaculture, tilapia farming is prone to microbiological risks as various pathogenic bacteria may proliferate in the anthropogenic environment (Grande Burgos et al., 2018). One of the common pathogenic bacteria infecting cultured fish is *Pseudomonas* species, where most of them are known as opportunistic pathogens with diverse antibiotic resistance mechanisms (Duman et al., 2021; Pang et al., 2019). Here, we isolated and characterized the *P. otitidis* NK1, a novel strain of *P. otitidis* species, and a novel *Pseudomonas* phage, PotUPM1 from tilapia fish during an outbreak. Initially identified as *P. aeruginosa*, the isolated bacterial strain was found to be *P. otitidis* after whole genome sequencing. Cases of *P. otitidis* misidentification are relatively common in the clinical setting, unless molecular identification methods are used (Alqurashi et al., 2022; Caixinha et al., 2021). Due to the phenotypic similarities between *P. otitidis* and *P. aeruginosa,* the occurrence of *P. otitidis* and its clinical and environmental impact especially in aquaculture may be largely underestimated. Although *P. otitidis* is known as an opportunistic pathogen, earlier studies had shown that a non-pathogenic *P. otitidis* strain isolated from marine fish, *M. seheli* can potentially be used as a potent indigenous probiotic in aquaculture (Husain et al., 2022). However, *P. otitidis* NK1 isolated from tilapia in this study was found to exhibit beta-hemolytic activity on blood agar, which indicates its potential pathogenicity in tilapia. To date, no *P. otitidis* strains with beta hemolytic properties have been isolated. However, there has been one alpha hemolytic *P. otitidis* strain reported, which was isolated from patients with chronic otitis media and had a similar antibiotic resistance profile to that of *P. otitidis* NK1 (Lee et al., 2012).

Based on genotypic characterization, *P. otitidis* NK1 has a metallo-β-lactamase (MBL) gene which is inherent in all isolated *P. otitidis* thus far (Thaller et al., 2011). MBL belongs to the broad-spectrum class B-lactamases that hydrolyze most β-lactam families, including carbapenems (Bush and Jacoby, 2010). In a previous study, *P. otitidis* appeared to be susceptible to piperacillin, ceftazidime, aztreonam, and gentamicin, while some strains were intermediate or resistant to carbapenems (Thaller et al., 2011). *P. otitidis* NK1 exhibited similar antibiotic resistant profile, but it showed decreased susceptibility to aztreonam unlike the previously characterized strains. As the $bla_{\text{POM-1}}$ antimicrobial resistance gene confers resistance only to carbapenems, penicillins, and cephalosporins, but not to aztreonam, the development of the acquired resistance to aztreonam in *P. otitidis* NK1 may be due to mutations in chromosomal genes or acquisition of external genetic

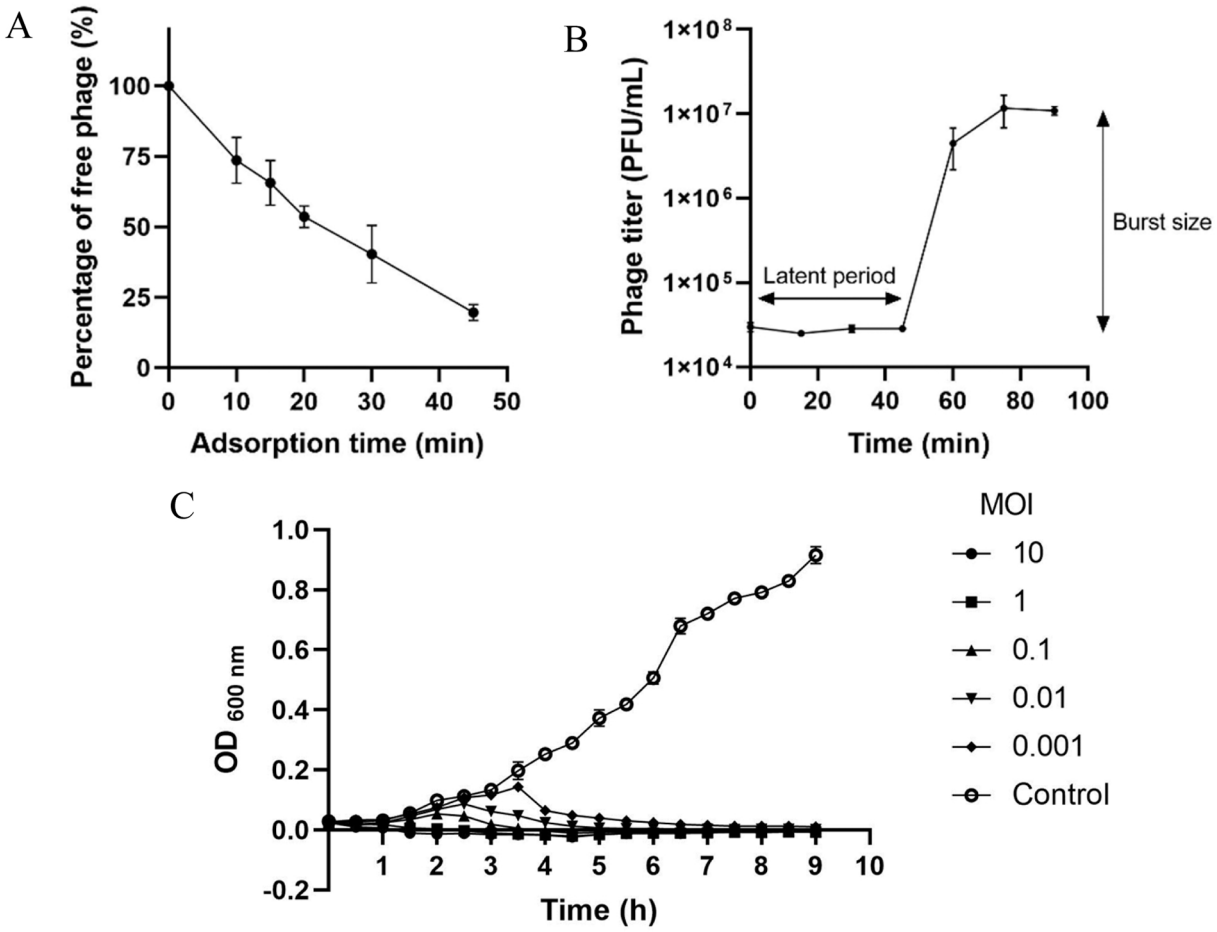

Fig. 5. Growth kinetics of phage and lysis profile of phage PotUPM1. **(A)** The adsorption curve showed the percentage of free phage particles remained at certain timepoints up to 45 min; **(B)** The one-step growth curve showed one cycle of phage growth with latent period of 52 min and a burst size of 405 PFU/cell; **(C)** The lysis profile in bacterial killing assay shown a reduction in turbidity measurement of phage infected host cells up to 9th hour of post-inoculation. Data are presented as mean ± SD of three independent experiments.

resistance determinant from other organisms present in the environment (Munita and Arias, 2016). *P. otitidis* NK1 was also non-susceptible to tetracycline, which is consistent with *P. otitidis* DSM 17224 (Clark et al., 2006). Although tetracycline is not listed in the CLSI breakpoints for *P. aeruginosa*, it was still tested in this study to compare the results of antibiotic susceptibility testing with the first characterized *P. otitidis* strain (Clark et al., 2006). However, the antimicrobial susceptibility test in this study was only performed using the disc diffusion assay, thus a susceptibility test using dilution methods to determine its MIC can further confirm this.

To date, there are only four complete genome assemblies of *P. otitidis* strains available in the Genbank database. *P. otitidis* NK1 showed more than 97 % ANI to all four strains of *P. otitidis*. The highest ANI value was shown by *P. otitidis* BC12 (GCA_026651425.1), which was isolated from river water in Ghana. Identification of putative virulent determinants through VFDB server revealed various bacterial virulent components such as flagella, type IV pili, alginate, capsular polysaccharides, phospholipase C, protease, pyoverdine, regulation and secretion systems, phytotoxin, and efflux pump that provide diverse effects in the microbial pathogenesis. The predicted MtrCDE efflux pump has so far been found only in *Neisseria gonorrhoeae* and never in any *Pseudomonas* bacteria (Tamburrino et al., 2017). The variety of resistance and virulent genes observed in the genome of *P. otitidis* NK1 indicates its potential pathogenicity and severity of infections on human, animals and plants. In addition to its beta-hemolytic properties on blood agar, the signs of pathogenicity shown by *P. otitidis* NK1 led to the attempt to isolate phages as an antimicrobial approach in this study.

The same fish sample was used for the isolation of phages due to the basic rule that phages are generally present in any source where their hosts are found (van Charante et al., 2021). Phage PotUPM1 was successfully isolated from the same tilapia sample obtained for bacterial host isolation from a fish farm in Malaysia. Clear plaques with turbid edges were formed on the double-layer agar, indicating that the host was fully susceptible to the phage, but the cells at the edges of the plaque were not yet fully lysed (Gallet et al., 2011). The TEM findings and whole genome sequencing analysis classified phage PotUPM1 as a member of *Siphoviridae* in the order of *Caudovirales* based on the phage morphology and genome composition as described by International Committee on the Taxonomy Viruses (ICTV) (Chibani et al., 2019). The genome annotation of phage PotUPM1 revealed a phage integrase gene, and the lifestyle prediction through PhageLeads server confirmed that it is a temperate phage capable of integrating its own genome into that of its host. However, the lysogenic efficiency of phage PotUPM1 on *P. otitidis* NK1 calculated was 0 %. These suggested that phage PotUPM1 underwent lytic interaction with its host under normal laboratory propagation conditions. The activation of a lytic cycle is favored when there is a large number of bacteria, and the progeny phage tends to become dormant and enter the lysogenic cycle when the hosts are limited (Doss et al., 2017). This may explain the lytic preference of phage PotUPM1 under laboratory cultivation conditions, as the host was supplied at high concentrations compared to the natural environment.

Based on the nucleotide comparison of phage whole genome on

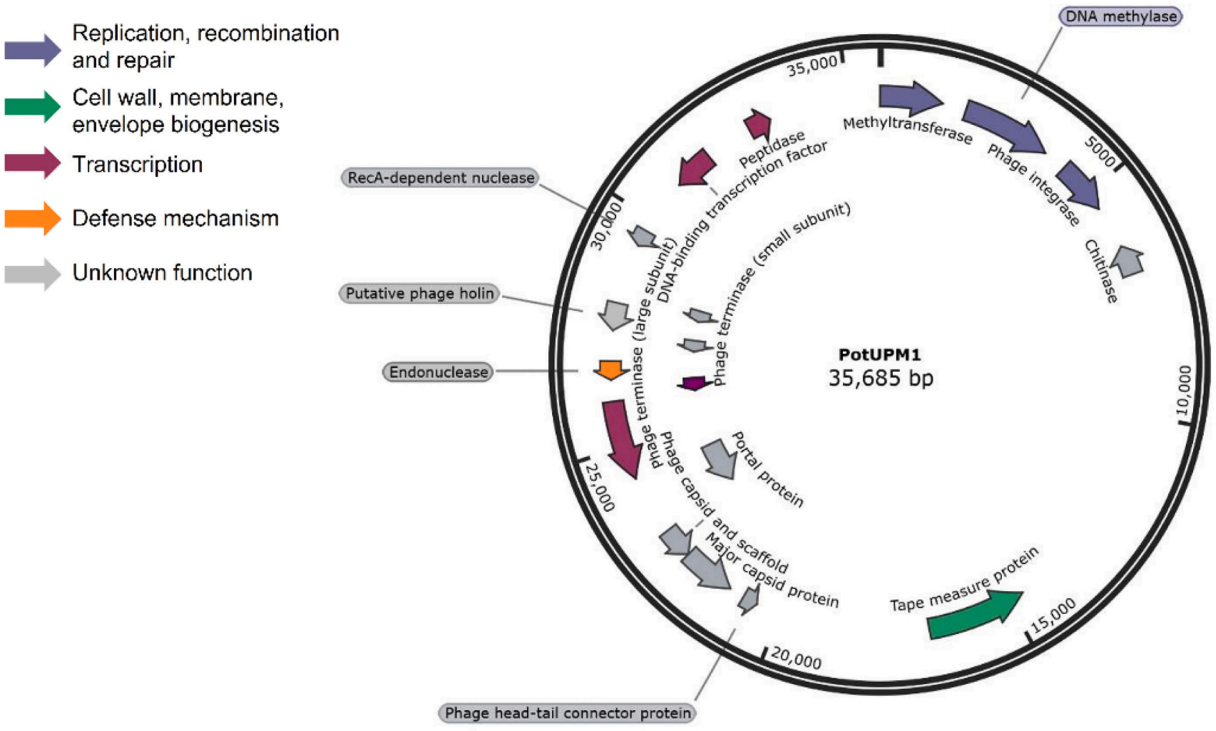

Fig. 6. A circular genome map of PotUPM1 generated using SnapGene software. Predicted ORFs annotated by eggNOG-mapper are represented by arrows, where the arrowheads indicate the orientation of the respective ORFs. Different COGs functional groups are denoted by different colours according to their category. Only ORFs assigned with functional groups and annotated functions are shown.

BLASTn, the evolutionary relationship between phage PotUPM1 and other reported *Pseudomonas* phages was evaluated. Phage PotUPM1 is a novel phage, and most related to three phages of *P. aeruginosa*; these include *Pseudomonas* phage LKA5, isolated in Belgium (Pourcel et al., 2017), *Pseudomonas* phage PP9W, isolated in China (Long et al., 2022), and *Pseudomonas* phage Dobby, isolated in United States (Johnson et al., 2019), and all are temperate phages. Nevertheless, the highest similarity was only at 83.54 %, which is not surprising since there has not been any *P. otitidis* phages described so far. Genome annotation revealed a large portion (64.15 %) of phage PotUPM1 genome as hypothetical proteins of unknown functions, which is a common problem in phage studies. An accumulation of numerous proteins with unknown function in the databases was observed due to the increasing gap between predicted phage gene sequences and their respective functions (Mohanraj et al., 2019).

In general, the properties of phage PotUPM1 as a temperate phage makes it an unsuitable candidate for phage therapy because of its tendency to alter the host phenotype and mediate gene transfers between bacteria that may increase bacterial virulence (Borodovich et al., 2022; Doss et al., 2017). However, its high lytic activity, the absence of harmful genes and its stability across a wide range of temperature and pH make it worthy of further genetic engineering studies. Temperate phages can be genetically engineered to become strictly lytic phages by eliminating genes involved in the lysogenic lifecycle (Kilcher et al., 2018), and can be used as gene delivery vehicles for DNA-encoded vaccines or antibacterial treatments (Park et al., 2017; Yosef et al., 2015). In addition, instead of using whole phages, phage lytic proteins can also be used for antibacterial treatment. Examples of phage proteins involved in host lysis are endolysins, virion-associated peptidoglycan hydrolases (VAPGH), polysaccharide depolymerases, and holins. Phage PotUPM1 was found to encode an endolysin from the glycoside hydrolase family 19 (ORF8) and two holins (ORF 35 and 36), which can be used as potential enzybiotics for antibacterial treatments. In summary, phage vB_PotS-PotUPM1 is a novel isolated temperate phage targeting *P. otitidis* NK1 isolated from tilapia. As far as to our knowledge, this is the first report of a *P. otitidis* phage. The absence of virulence genes and high stability reflect the engineering potential of phage PotUPM1 to eliminate the lysogeny-associated genes that diminish the therapeutic potential of this phage. The properties of the phage indicated that it could be a good candidate for genetic engineering for therapeutic and biocontrol purposes. The characterized phage in this study could contribute to the development of new phage therapy strategies for the emerging pathogen, *P. otitidis* especially in the aquaculture industry.

Funding

This work was supported by Ministry of Higher Education under Fundamental Research Grant Scheme (Project code: FRGS/1/2023/STG01/UPM/02/29) and Geran Inisiatif Putra Siswazah, Universiti Putra Malaysia (Project code: GP-IPS/2022/9728000).

CRediT authorship contribution statement

Methodology, investigation, formal analysis, writing – original draft, A.N.T.; methodology, investigation, M.H.M.M.K.; conceptualization, supervision, writing – review & editing, C.M.C., M.S.M.A., K.Y., H.C.Y. H.M.G and A.A.L.S. All authors have read and agreed to the published version of the manuscript.

Declaration of Competing Interest

The authors declare that they have no known competing financial interests or personal relationships that could have appeared to influence the work reported in this paper.

Data Availability

The complete genome sequences of *P. otitidis* NK1 and phage PotUPM1 were deposited in the NCBI database under accession number

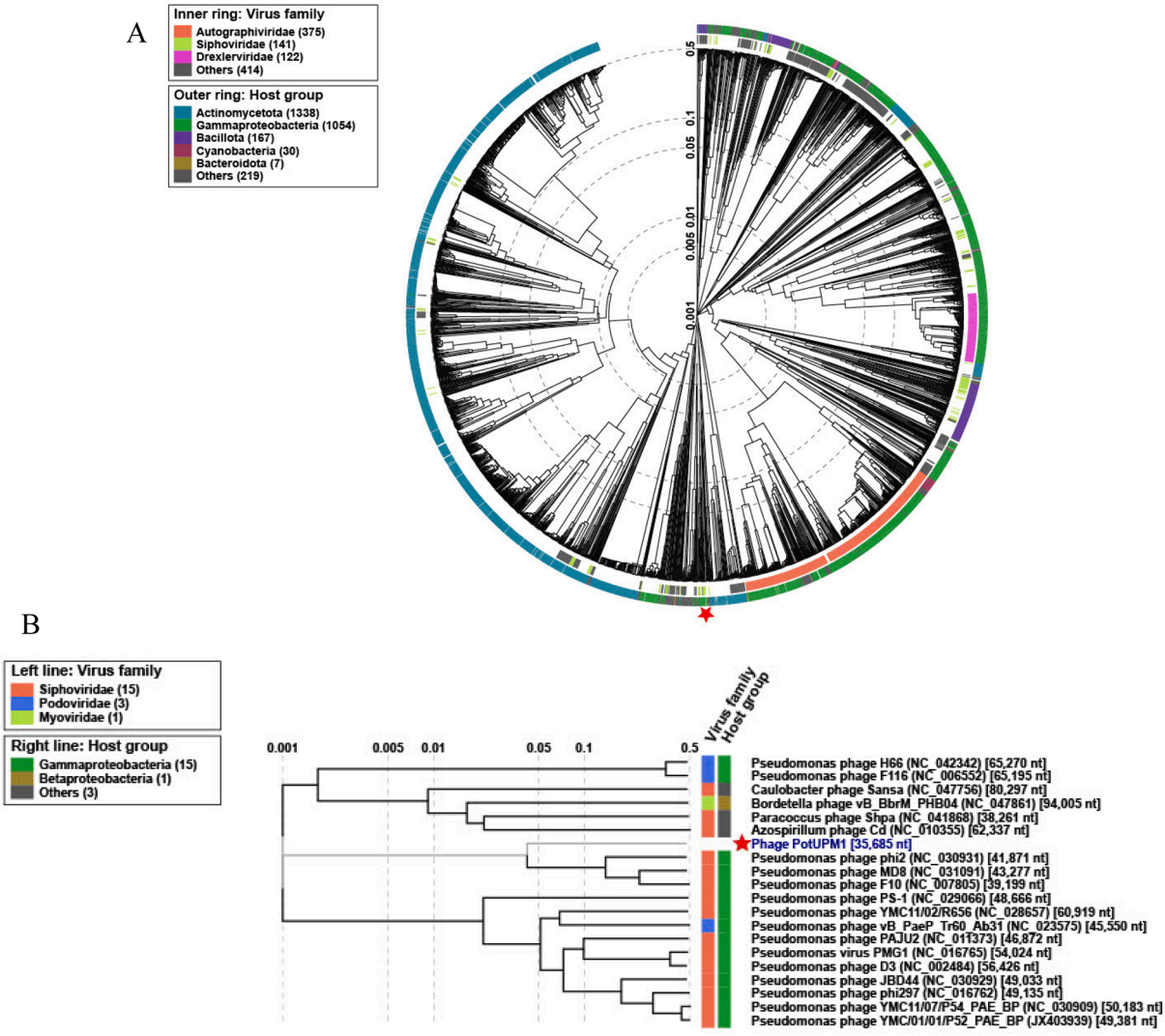

Fig. 7. Comparative genomic analysis of PotUPM1 based on the viral proteome. The branch represented phage PotUPM1 is denoted by a red star. **(A)** Viral proteomic tree represented in circular view. The rings represent the virus families (inner ring) and host groups (outer ring). Branch lengths are based on log-scaling; **(B)** Viral phylogenetic tree represented in rectangular view with 20 phage genome sequences. A total of 19 phage sequences with the nearest S_G score to PotUPM1 were selected for comparison.

of JARGCP000000000 and OQ633420, respectively.

Appendix A. Supporting information

Supplementary data associated with this article can be found in the online version at doi:10.1016/j.aqrep.2023.101883.

References

Ackermann, H.W., 2012. Bacteriophage electron microscopy. Adv. Virus Res. 82, 1–32. https://doi.org/10.1016/B978-0-12-394621-8.00017-0.

Adriaenssens, E.M., Brister, J.R., 2017. How to name and classify your phage: an informal guide. Viruses 9 (4), 70. https://doi.org/10.3390/v9040070.

Ahn, K.-J., 2018. Antibiotic production of *Pseudomonas otitidis* PS and mode of action. Microbiol. Biotechnol. Lett. 46 (1), 40–44. https://doi.org/10.4014/mbl.1712.12004.

Alcock, B.P., Raphenya, A.R., Lau, T.T.Y., Tsang, K.K., Bouchard, M., Edalatmand, A., Huynh, W., Nguyen, A.V., Cheng, A.A., Liu, S., Min, S.Y., Miroshnichenko, A., Tran, H.K., Werfalli, R.E., Nasir, J.A., Oloni, M., Speicher, D.J., Florescu, A., Singh, B., Faltyn, M., Hernandez-Koutoucheva, A., Sharma, A.N., Bordeleau, E., Pawlowski, A.C., Zubyk, H.L., Dooley, D., Griffiths, E., Maguire, F., Winsor, G.L., Beiko, R.G., Brinkman, F.S.L., Hsiao, W.W.L., Domselaar, G.V., McArthur, A.G., 2020. CARD 2020: antibiotic resistome surveillance with the comprehensive antibiotic resistance database. Nucleic Acids Res. 48 (D1), D517–D525. https://doi.org/10.1093/nar/gkz935.

Almpanis, A., Swain, M., Gatherer, D., McEwan, N., 2018. Correlation between bacterial G+ C content, genome size and the G+ C content of associated plasmids and bacteriophages. Micro Genom. 4 (4) https://doi.org/10.1099/mgen.0.000168.

Alqurashi, M., Alsaedy, A., Alalwan, B., Alzayer, M., Alswaji, A., Okdah, L., Doumith, M., Zowawi, H., Aljohani, S., Alghoribi, M., 2022. Epididymo-orchitis caused by POM-1 metallo-beta-lactamase-producing *Pseudomonas otitidis* in an immunocompetent patient: case report and molecular characterization. Pathogens 11 (12). https://doi.org/10.3390/pathogens11121475.

Belcaid, M., Bergeron, A., Poisson, G., 2011. The evolution of the tape measure protein: units, duplications and losses. Suppl 9(Suppl 9). BMC Bioinform 12, S10. https://doi.org/10.1186/1471-2105-12-S9-S10.

Borodovich, T., Shkoporov, A.N., Ross, R.P., Hill, C., 2022. Phage-mediated horizontal gene transfer and its implications for the human gut microbiome. Gastroenterol. Rep. 10, goac012 https://doi.org/10.1093/gastro/goac012.

Bortolaia, V., Kaas, R.S., Ruppe, E., Roberts, M.C., Schwarz, S., Cattoir, V., Philippon, A., Allesoe, R.L., Rebelo, A.R., Florensa, A.F., Fagelhauer, L., Chakraborty, T., Neumann, B., Werner, G., Bender, J.K., Stingl, K., Nguyen, M., Coppens, J., Xavier, B. B., Malhotra-Kumar, S., Westh, H., Pinholt, M., Anjum, M.F., Duggett, N.A., Kempf, I., Nykasenoja, S., Olkkola, S., Wieczorek, K., Amaro, A., Clemente, L., Mossong, J., Losch, S., Ragimbeau, C., Lund, O., Aarestrup, F.M., 2020. ResFinder 4.0 for predictions of phenotypes from genotypes. J. Antimicrob. Chemother. 75 (12), 3491–3500. https://doi.org/10.1093/jac/dkaa345.

Bush, K., Jacoby, G.A., 2010. Updated functional classification of beta-lactamases. Antimicrob. Agents Chemother. 54 (3), 969–976. https://doi.org/10.1128/AAC.01009-09.

Caixinha, A.L., Valsamidis, A.N., Chen, M., Lindberg, M., 2021. *Pseudomonas otitidis* bacteraemia in a patient with COPD and recurrent pneumonia: case report and

literature review. BMC Infect. Dis. 21 (1), 868 https://doi.org/10.1186/s12879-021-06569-8.
Cantalapiedra, C.P., Hernández-Plaza, A., Letunic, I., Bork, P., Huerta-Cepas, J., 2021. eggNOG-mapper v2: functional annotation, orthology assignments, and domain prediction at the metagenomic scale. Mol. Biol. Evol. 38 (12), 5825–5829. https://doi.org/10.1093/molbev/msab293.
Chegini, Z., Khoshbayan, A., Taati Moghadam, M., Farahani, I., Jazireian, P., Shariati, A., 2020. Bacteriophage therapy against *Pseudomonas aeruginosa* biofilms: a review. Ann. Clin. Microbiol. Antimicrob. 19 (1), 45 https://doi.org/10.1186/s12941-020-00389-5.
Chibani, C.M., Farr, A., Klama, S., Dietrich, S., Liesegang, H., 2019. Classifying the unclassified: a phage classification method. Viruses 11 (2). https://doi.org/10.3390/v11020195.
Clark, L.L., Dajcs, J.J., McLean, C.H., Bartell, J.G., Stroman, D.W., 2006. *Pseudomonas otitidis* sp. nov., isolated from patients with otic infections. Int J. Syst. Evol. Microbiol. 56 (Pt 4), 709–714. https://doi.org/10.1099/ijs.0.63753-0.
Clokie, M.R., Kropinski, A.M., Lavigne, R., 2009. Bacteriophages. Humana Press, Totowa.
CLSI, 2021. Performance standards for antimicrobial susceptibility testing, 31st ed. Clinical and Laboratory Standards Institute, USA.
Cross, T., Schoff, C., Chudoff, D., Graves, L., Broomell, H., Terry, K., Farina, J., Correa, A., Shade, D., Dunbar, D., 2015. An optimized enrichment technique for the isolation of Arthrobacter bacteriophage species from soil sample isolates. JoVE (98), e52781. https://doi.org/10.3791/52781.
Davis, J.J., Wattam, A.R., Aziz, R.K., Brettin, T., Butler, R., Butler, R.M., Chlenski, P., Conrad, N., Dickerman, A., Dietrich, E.M., 2020. The PATRIC bioinformatics resource center: expanding data and analysis capabilities. Nucleic Acids Res. 48 (D1), D606–D612. https://doi.org/10.1093/nar/gkz943.
Decewicz, P., Golec, P., Szymczak, M., Radlinska, M., Dziewit, L., 2020. Identification and characterization of the first virulent phages, including a novel jumbo virus, infecting *Ochrobactrum* spp. Int. J. Mol. Sci. 21 (6) https://doi.org/10.3390/ijms21062096.
Doss, J., Culbertson, K., Hahn, D., Camacho, J., Barekzi, N., 2017. A review of phage therapy against bacterial pathogens of aquatic and terrestrial organisms. Viruses 9 (3). https://doi.org/10.3390/v9030050.
Duman, M., Mulet, M., Altun, S., Saticioglu, I.B., Ozdemir, B., Ajmi, N., Lalucat, J., García-Valdés, E., 2021. The diversity of *Pseudomonas* species isolated from fish farms in Turkey. Aquaculture 535, 736369. https://doi.org/10.1016/j.aquaculture.2021.736369.
Gallet, R., Kannoly, S., Wang, I.N., 2011. Effects of bacteriophage traits on plaque formation. BMC Microbiol. 11, 181. https://doi.org/10.1186/1471-2180-11-181.
García-Ulloa, M.I., Escalante, A.E., Moreno-Letelier, A., Eguiarte, L.E., Souza, V., 2021. Evolutionary rescue of an environmental *Pseudomonas otitidis* in response to anthropogenic perturbation. Front. Microbiol. 11, 563885 https://doi.org/10.3389/fmicb.2020.563885.
Ghose, C., Euler, C.W., 2020. Gram-negative bacterial lysins. Antibiotics (Basel) 9 (2). https://doi.org/10.3390/antibiotics9020074.
Girard, L., Lood, C., Hofte, M., Vandamme, P., Rokni-Zadeh, H., van Noort, V., Lavigne, R., De Mot, R., 2021. The ever-expanding *Pseudomonas* genus: description of 43 new species and partition of the *Pseudomonas putida* group. Microorganisms 9 (8). https://doi.org/10.3390/microorganisms9081766.
Grande Burgos, M.J., Romero, J.L., Perez Pulido, R., Cobo Molinos, A., Galvez, A., Lucas, R., 2018. Analysis of potential risks from the bacterial communities associated with air-contact surfaces from tilapia (*Oreochromis niloticus*) fish farming. Environ. Res. 160, 385–390. https://doi.org/10.1016/j.envres.2017.10.021.
Green, M.R., Sambrook, J., 2017. Isolation of high-molecular-weight DNA using organic solvents. pdb prot093450 Cold Spring Harb. Protoc. 2017 (4). https://doi.org/10.1101/pdb.prot093450.
Harada, L.K., Silva, E.C., Campos, W.F., Del Fiol, F.S., Vila, M., Dąbrowska, K., Krylov, V. N., Balcão, V.M., 2018. Biotechnological applications of bacteriophages: state of the art. Microbiol. Res. 212, 38–58. https://doi.org/10.1016/j.micres.2018.04.007.
Husain, F., Duraisamy, S., Balakrishnan, S., Ranjith, S., Chidambaram, P., Kumarasamy, A., 2022. Phenotypic assessment of safety and probiotic potential of native isolates from marine fish *Moolgarda seheli* towards sustainable aquaculture. Biol. (Bratisl.) 77 (3), 775–790. https://doi.org/10.1007/s11756-021-00957-w.
Hyman, P., Abedon, S.T., 2009. Practical methods for determining phage growth parameters. Bacteriophages: methods and protocols, volume 1: isolation, characterization, and interactions, 175–202.
Ibrahim, A.G., Abd Elsalam, H.E., 2018. Enhancement the biodegradation of sodium dodecyl sulfate by *Pseudomonas aeruginosa* and *Pseudomonas otitidis* isolated from waste water in Saudi Arabia. Annu. Res. Rev. Biol. 1–7. https://doi.org/10.9734/ARRB/2018/43744.
Jing, W., Byung-Gil, J., Kyoung-Sook, K., Young-Choon, L., Nak-Chang, S., 2009. Isolation and characterization of *Pseudomonas otitidis* WL-13 and its capacity to decolorize triphenylmethane dyes. J. Environ. Sci. 21 (7), 960–964. https://doi.org/10.1016/s1001-0742(08)62368-2.
Johnson, G., Wolfe, A.J., Putonti, C., 2019. Characterization of the φCTX-like *Pseudomonas aeruginosa* phage Dobby isolated from the kidney stone microbiota. Access Microbiol. 1 (1), e000002 https://doi.org/10.1099/acmi.0.000002.
Kilcher, S., Studer, P., Muessner, C., Klumpp, J., Loessner, M.J., 2018. Cross-genus rebooting of custom-made, synthetic bacteriophage genomes in L-form bacteria. Proc. Natl. Acad. Sci. U. S. A. 115 (3), 567–572. https://doi.org/10.1073/pnas.1714658115.
Kim, D., Hong, S.K., Seo, Y.H., Kim, M.S., Kim, H.S., Yong, D., Jeong, S.H., Lee, K., Chong, Y., 2016. Two non-otic cases of POM-1 metallo-beta-lactamase-producing *Pseudomonas otitidis* infection: necrotizing fasciitis and pan-peritonitis. J. Glob. Antimicrob. Resist 7, 157–158. https://doi.org/10.1016/j.jgar.2016.09.006.
Kolmogorov, M., Yuan, J., Lin, Y., Pevzner, P.A., 2019. Assembly of long, error-prone reads using repeat graphs. Nat. Biotechnol. 37 (5), 540–546. https://doi.org/10.1038/s41587-019-0072-8.
Kropinski, A.M., 2009. Measurement of the rate of attachment of bacteriophage to cells, in: Clokie, M.R.J., Kropinski, A.M. (Eds.), Bacteriophages: methods and protocols, volume 1: isolation, characterization, and Interactions. Humana Press, Totowa, pp. 151–155.
Kwiatek, M., Parasion, S., Rutyna, P., Mizak, L., Gryko, R., Niemcewicz, M., Olender, A., Łobocka, M., 2017. Isolation of bacteriophages and their application to control *Pseudomonas aeruginosa* in planktonic and biofilm models. Res. Microbiol. 168 (3), 194–207. https://doi.org/10.1016/j.resmic.2016.10.009.
Lee, K., Kim, C., Yong, D., Yum, J., Chung, M., Chong, Y., Thaller, M., Rossolini, G., 2012. POM-1 metallo-β-lactamase–producing *Pseudomonas otitidis* isolate from a patient with chronic otitis media. Diagn. Microbiol. Infect. Dis. 72 (3), 295–296. https://doi.org/10.1016/j.diagmicrobio.2011.11.007.
Lerdsittikul, V., Thongdee, M., Chaiwattanarungruengpaisan, S., Atithep, T., Apiratwarrasakul, S., Withatanung, P., Clokie, M.R., Korbsrisate, S., 2022. A novel virulent *Litunavirus* phage possesses therapeutic value against multidrug resistant *Pseudomonas aeruginosa*. Sci. Rep. 12 (1), 21193 https://doi.org/10.1038/s41598-022-25576-6.
Liu, B., Zheng, D., Zhou, S., Chen, L., Yang, J., 2022. VFDB 2022: a general classification scheme for bacterial virulence factors. Nucleic Acids Res. 50 (D1), D912–D917. https://doi.org/10.1093/nar/gkab1107.
Long, X., Zhang, H., Wang, X., Mao, D., Wu, W., Luo, Y., 2022. RecT affects prophage lifestyle and host core cellular processes in *Pseudomonas aeruginosa*. Appl. Environ. Microbiol. 88 (18), e0106822 https://doi.org/10.1128/aem.01068-22.
Miyazaki, K., Hase, E., Maruya, T., 2020. Complete genome sequence of *Pseudomonas otitidis* strain MrB4, isolated from Lake Biwa in Japan. Microbiol. Resour. Announc. 9 (16), e00148–00120. https://doi.org/10.1128/MRA.00148-20.
Mohanraj, U., Wan, X., Spruit, C.M., Skurnik, M., Pajunen, M.I., 2019. A toxicity screening approach to identify bacteriophage-encoded anti-microbial proteins. Viruses 11 (11). https://doi.org/10.3390/v11111057.
Munita, J.M., Arias, C.A., 2016. Mechanisms of antibiotic resistance. Microbiol. Spectr. 4 (2) https://doi.org/10.1128/microbiolspec.VMBF-0016-2015.
Naguib, M.M., Khairalla, A.S., El-Gendy, A.O., Elkhatib, W.F., 2019. Isolation and characterization of mercury-resistant bacteria from wastewater sources in Egypt. Can. J. Microbiol. 65 (4), 308–321. https://doi.org/10.1139/cjm-2018-0379.
Nasr Azadani, D., Zhang, D., Hatherill, J.R., Silva, D., Turner, J.W., 2020. Isolation, characterization, and comparative genomic analysis of a phage infecting high-level aminoglycoside-resistant (HLAR) *Enterococcus faecalis*. PeerJ 8, e9171. https://doi.org/10.7717/peerj.9171.
Nishimura, Y., Yoshida, T., Kuronishi, M., Uehara, H., Ogata, H., Goto, S., 2017. ViPTree: the viral proteomic tree server. Bioinformatics 33 (15), 2379–2380. https://doi.org/10.1093/bioinformatics/btx157.
Overbeek, R., Olson, R., Pusch, G.D., Olsen, G.J., Davis, J.J., Disz, T., Edwards, R.A., Gerdes, S., Parrello, B., Shukla, M., Vonstein, V., Wattam, A.R., Xia, F., Stevens, R., 2014. The SEED and the rapid annotation of microbial genomes using subsystems technology (RAST). Nucleic Acids Res. 42 (Database issue), D206–D214. https://doi.org/10.1093/nar/gkt1226.
Pang, Z., Raudonis, R., Glick, B.R., Lin, T.J., Cheng, Z., 2019. Antibiotic resistance in *Pseudomonas aeruginosa*: mechanisms and alternative therapeutic strategies. Biotechnol. Adv. 37 (1), 177–192. https://doi.org/10.1016/j.biotechadv.2018.11.013.
Park, J.Y., Moon, B.Y., Park, J.W., Thornton, J.A., Park, Y.H., Seo, K.S., 2017. Genetic engineering of a temperate phage-based delivery system for CRISPR/Cas9 antimicrobials against *Staphylococcus aureus*. Sci. Rep. 7, 44929 https://doi.org/10.1038/srep44929.
Pourcel, C., Midoux, C., Hauck, Y., Vergnaud, G., Latino, L., 2017. Large preferred region for packaging of bacterial DNA by phiC725A, a novel *Pseudomonas aeruginosa* F116-Like bacteriophage. PLoS One 12 (1), e0169684. https://doi.org/10.1371/journal.pone.0169684.
Richter, M., Rossello-Mora, R., Oliver Glockner, F., Peplies, J., 2016. JSpeciesWS: a web server for prokaryotic species circumscription based on pairwise genome comparison. Bioinformatics 32 (6), 929–931. https://doi.org/10.1093/bioinformatics/btv681.
Rogovski, P., Cadamuro, R.D., da Silva, R., de Souza, E.B., Bonatto, C., Viancelli, A., Michelon, W., Elmahdy, E.M., Treichel, H., Rodríguez-Lázaro, D., 2021. Uses of bacteriophages as bacterial control tools and environmental safety indicators. Front. Microbiol. 12, 3756. https://doi.org/10.3389/fmicb.2021.793135.
Roland, P.S., Stroman, D.W., 2002. Microbiology of acute otitis externa. Laryngoscope 112 (7 Pt 1), 1166–1177. https://doi.org/10.1097/00005537-200207000-00005.
Rose, S., Hill, R., Bermudez, L.E., Miller-Morgan, T., 2013. Imported ornamental fish are colonized with antibiotic-resistant bacteria. J. Fish. Dis. 36 (6), 533–542. https://doi.org/10.1111/jfd.12044.
Saber, F.M., Abdelhafez, A.A., Hassan, E.A., Ramadan, E.M., 2015. Characterization of fluorescent pseudomonads isolates and their efficiency on the growth promotion of tomato plant. Ann. Agric. Sci. 60 (1), 131–140. https://doi.org/10.1016/j.aoas.2015.04.007.
Sarjito, S., Ariyati, R.W., Desrina, D., Haditomo, A.C., Budiarjo, A., Sabdaningsih, A., Pravitno, S.B., 2022. Molecular identification of causative bacterial disease in giant gourami (*Osphronemus goramy*) based on 16S rRNA gene from extensive fishpond in Banjarnegara Regency, Indonesia. Egypt. J. Aquat. Biol. Fish. 26 (6), 555–566. https://doi.org/10.21608/ejabf.2022.273446.
Singh, P., Tiwary, B.N., 2016. Isolation and characterization of glycolipid biosurfactant produced by a *Pseudomonas otitidis* strain isolated from Chirimiri coal mines, India. Bioresour. Bioprocess 3 (42), 1–16. https://doi.org/10.1186/s40643-016-0119-3.

Tamburrino, G., Llabres, S., Vickery, O.N., Pitt, S.J., Zachariae, U., 2017. Modulation of the *Neisseria gonorrhoeae* drug efflux conduit MtrE. Sci. Rep. 7 (1), 17091 https://doi.org/10.1038/s41598-017-16995-x.

Tan, H., Zhang, Z., Hu, Y., Wu, L., Liao, F., He, J., Luo, B., He, Y., Zuo, Z., Ren, Z., 2015. Isolation and characterization of Pseudomonas otitidis TH-N1 capable of degrading Zearalenone. Food Control 47, 285–290. https://doi.org/10.1016/j.foodcont.2014.07.013.

Thaller, M.C., Borgianni, L., Di Lallo, G., Chong, Y., Lee, K., Dajcs, J., Stroman, D., Rossolini, G.M., 2011. Metallo-beta-lactamase production by *Pseudomonas otitidis*: a species-related trait. Antimicrob. Agents Chemother. 55 (1), 118–123. https://doi.org/10.1128/AAC.01062-10.

Thulasinathan, B., Nainamohamed, S., Samuel, J.O.E., Soorangkattan, S., Muthuramalingam, J., Kulanthaisamy, M., Balasubramani, R., Nguyen, D.D., Chang, S.W., Bolan, N., 2019. Comparative study on *Cronobacter sakazakii* and *Pseudomonas otitidis* isolated from septic tank wastewater in microbial fuel cell for bioelectricity generation. Fuel 248, 47–55. https://doi.org/10.1016/j.fuel.2019.03.060.

van Charante, F., Holtappels, D., Blasdel, B., Burrowes, B.H., 2021. Isolation of bacteriophages. In: Harper, D.R., Abedon, S.T., Burrowes, B.H., McConville, M.L. (Eds.), Bacteriophages. Springer, Cham, pp. 433–464.

Walker, B.J., Abeel, T., Shea, T., Priest, M., Abouelliel, A., Sakthikumar, S., Cuomo, C.A., Zeng, Q., Wortman, J., Young, S.K., Earl, A.M., 2014. Pilon: an integrated tool for comprehensive microbial variant detection and genome assembly improvement. PLoS One 9 (11), e112963. https://doi.org/10.1371/journal.pone.0112963.

Wick, R.R., Judd, L.M., Gorrie, C.L., Holt, K.E., 2017. Unicycler: resolving bacterial genome assemblies from short and long sequencing reads. PLoS Comput. Biol. 13 (6), e1005595 https://doi.org/10.1371/journal.pcbi.1005595.

Wong, M.H., Chan, E.W., Chen, S., 2015. Isolation of carbapenem-resistant *Pseudomonas* spp. from food. J. Glob. Antimicrob. Resist 3 (2), 109–114. https://doi.org/10.1016/j.jgar.2015.03.006.

Yosef, I., Manor, M., Kiro, R., Qimron, U., 2015. Temperate and lytic bacteriophages programmed to sensitize and kill antibiotic-resistant bacteria. Proc. Natl. Acad. Sci. U. S. A. 112 (23), 7267–7272. https://doi.org/10.1073/pnas.1500107112.

Yukgehnaish, K., Rajandas, H., Parimannan, S., Manickam, R., Marimuthu, K., Petersen, B., Clokie, M.R.J., Millard, A., Sicheritz-Ponten, T., 2022. PhageLeads: rapid assessment of phage therapeutic suitability using an ensemble machine learning approach. Viruses 14 (2). https://doi.org/10.3390/v14020342.

Zhang, L., Xu, D., Huang, Y., Zhu, X., Rui, M., Wan, T., Zheng, X., Shen, Y., Chen, X., Ma, K., Gong, Y., 2017. Structural and functional characterization of deep-sea thermophilic bacteriophage GVE2 HNH endonuclease. Sci. Rep. 7, 42542 https://doi.org/10.1038/srep42542.